Lyapunov Exponent and Out-of-Time-Ordered Correlator's Growth Rate in a Chaotic System

Efim B. Rozenbaum,[1,2,*] Sriram Ganeshan,[3,2] and Victor Galitski[1,2,4]
[1]*Joint Quantum Institute, University of Maryland, College Park, Maryland 20742, USA*
[2]*Condensed Matter Theory Center, Department of Physics, University of Maryland, College Park, Maryland 20742, USA*
[3]*Simons Center of Geometry and Physics, Stony Brook, New York 11794, USA*
[4]*School of Physics and Astronomy, Monash University, Melbourne, Victoria 3800, Australia*
(Received 27 September 2016; published 21 February 2017)

It was proposed recently that the out-of-time-ordered four-point correlator (OTOC) may serve as a useful characteristic of quantum-chaotic behavior, because, in the semiclassical limit $\hbar \to 0$, its rate of exponential growth resembles the classical Lyapunov exponent. Here, we calculate the four-point correlator $C(t)$ for the classical and quantum kicked rotor—a textbook driven chaotic system—and compare its growth rate at initial times with the standard definition of the classical Lyapunov exponent. Using both quantum and classical arguments, we show that the OTOC's growth rate and the Lyapunov exponent are, in general, distinct quantities, corresponding to the logarithm of the phase-space averaged divergence rate of classical trajectories and to the phase-space average of the logarithm, respectively. The difference appears to be more pronounced in the regime of low kicking strength K, where no classical chaos exists globally. In this case, the Lyapunov exponent quickly decreases as $K \to 0$, while the OTOC's growth rate may decrease much slower, showing a higher sensitivity to small chaotic islands in the phase space. We also show that the quantum correlator as a function of time exhibits a clear singularity at the Ehrenfest time t_E: transitioning from a time-independent value of $t^{-1} \ln C(t)$ at $t < t_E$ to its monotonic decrease with time at $t > t_E$. We note that the underlying physics here is the same as in the theory of weak (dynamical) localization [Aleiner and Larkin, Phys. Rev. B **54**, 14423 (1996); Tian, Kamenev, and Larkin, Phys. Rev. Lett. **93**, 124101 (2004)] and is due to a delay in the onset of quantum interference effects, which occur sharply at a time of the order of the Ehrenfest time.

DOI: 10.1103/PhysRevLett.118.086801

One of the central goals in the study of quantum chaos is to establish a correspondence principle between classical and quantum dynamics of classically chaotic systems [1–7]. Several previous works [7–11] have attempted to recover fingerprints of classical chaos in quantum dynamics. In particular, Aleiner and Larkin [12] showed the existence of a semiclassical "quantum chaotic" regime attributed to the delay in the onset of quantum effects (due to weak localization) revealing the key measure of classical chaos—the Lyapunov exponent (LE). Recently, the subject of quantum chaos has been revived by the discovery of an unexpected conjecture that puts a bound on the growth rate of an out-of-time-ordered four-point correlator (OTOC) [13,14]. The OTOC was first introduced by Larkin and Ovchinnikov to quantify the regime of validity of quasiclassical methods in the theory of superconductivity [15]. The growth rate of the OTOC appears to be closely related to the LE. Recent works have proposed experimental protocols to probe the OTOC in cold atom and cavity QED setups [16]. Several recent preprints have employed the OTOC as a probe to characterize many-body-localized systems [17].

In this Letter, we calculate the Lyapunov exponent, OTOC, and the two-point correlator for the quantum kicked rotor (QKR), which is a canonical driven model of quantum chaos [1,4,18]. The classical version of this model manifests a regular-to-chaotic transition (as a function of driving strength K) which enables us to benchmark the behavior of the OTOC against the presence and absence of classical chaos. We show that, in the limit of a small dimensionless effective Planck's constant, $\hbar_{\text{eff}} \to 0$, there exists a "quantum chaotic" regime [12,15] at early times where the OTOC, $C(t) = -\langle [\hat{p}(t), \hat{p}(0)]^2 \rangle$, grows exponentially. This correlator's growth rate $\tilde{\lambda}$, that we abbreviate for brevity as CGR, is found to be independent of the dimensionless Planck's constant $\hbar_{\text{eff}}$ and is purely classical at early times for the kicked rotor. Most importantly, the CGR and the standard definition of the LE in classical systems are shown to be different at all nonzero kicking strengths. In particular, for the classically regular regime $K < K_{\text{cr}}$, the CGR significantly exceeds the LE due to a much higher sensitivity to the presence of small chaotic islands. For the classically deeply chaotic regime $K \gg K_{\text{cr}}$, the CGR exceeds the LE by nearly a constant. We attribute these distinctions to different averaging procedures carried out to extract these exponents and posit that this statement may be more general than the specific QKR model studied here.

We also show that deviations from the essentially classical behavior of the OTOC, $C(t) \sim e^{2\tilde{\lambda}t}$, occur sharply at a time of the order of the Ehrenfest time t_E, where the OTOC exhibits a clear cusp. This corresponds to the minimal time it takes classical trajectories to self-intersect, indicating the onset of quantum interference effects [12]. This is in analogy to the weak dynamical localization discussed by Tian, Kamenev, and Larkin [19]. At longer times $t > t_E$, the quantum disordering effects subdue the exponential growth dictated by the CGR to a power-law growth.

Finally, we calculate the two-point correlation function and show that the CGR $\tilde{\lambda}$ is not revealed in this quantity (nor in the single-point average—e.g., the kinetic energy as has been well known [7]). However, we find that the two-point correlator does contain fingerprints of a classical transition from regular dynamics to chaos even deep in the quantum regime at long times, which has been a subject of long-standing theoretical and experimental interest [20–23].

Quantum kicked rotor.—The dimensionless Hamiltonian of the QKR [1,4,18] can be written as

$$\hat{H} = \frac{\hat{p}^2}{2} + K\cos(\hat{x})\Delta(t), \tag{1}$$

where $\Delta(t) = \sum_{j=-\infty}^{\infty} \delta(t-j)$ is the sum of δ pulses, $\hat{p}$ is the dimensionless angular-momentum operator, $\hat{x}$ is the angular coordinate operator, and t is the dimensionless time. The QKR is characterized by two parameters. One of them, the kicking strength K, comes from the classical kicked rotor (KR, also called the Chirikov standard map) [24]. Another parameter is the dimensionless effective Planck constant $\hbar_{\mathrm{eff}}$, which enters the dimensionless angular-momentum operator ($\hat{p} = -i\hbar_{\mathrm{eff}}(\partial/\partial x)$) and the dimensionless Schrödinger equation: $i\hbar_{\mathrm{eff}}(\partial/\partial t)|\Psi\rangle = \hat{H}|\Psi\rangle$. The eigenvalues of $\hat{p}$ are quantized in units of $\hbar_{\mathrm{eff}}$ due to the periodic boundary conditions. Note that, in the classical KR, the parameter $\hbar_{\mathrm{eff}}$ is absent. In order to understand how classical chaos emerges from quantum dynamics, we compute the OTOC and the two-point correlator in the regime of $\hbar_{\mathrm{eff}} \to 0$ at short time scales.

Lyapunov exponent and OTOC's growth rate (CGR).—To specify our quantum diagnostics for chaotic behavior in the QKR, we choose the OTOC $C(t)$ [14,15] and two-point correlator $B(t)$ as

$$C(t) = -\langle[\hat{p}(t), \hat{p}(0)]^2\rangle, \qquad B(t) = \mathrm{Re}\langle\hat{p}(t)\hat{p}(0)\rangle. \tag{2}$$

We point out that $C(t)$ is closely related to the Loschmidt echo (also known as fidelity). In the previous works, fidelity has been used as a theoretical and experimental diagnostic of quantum chaos [16,25–32].

Before carrying out quantum calculations, we consider the classical correspondence of $C(t)$ [14,15]. At short times $t < t_E$ [33],

$$C(t) = \hbar_{\mathrm{eff}}^2 \left\langle \left(\frac{\partial \hat{p}(t)}{\partial x(0)}\right)^2 \right\rangle \approx \hbar_{\mathrm{eff}}^2 \left\langle\!\!\left\langle \left(\frac{\Delta p(t)}{\Delta x(0)}\right)^2 \right\rangle\!\!\right\rangle = C_{\mathrm{cl}}(t), \tag{3}$$

where we changed the expectation value of the operator derivative to the finite differences of the classical variables averaged over the phase space ($\langle\langle \ldots \rangle\rangle$ denotes the classical phase-space average). Note that the averaging allows for a direct comparison of the classical $C_{\mathrm{cl}}(t)$ to the quantum $C(t)$. Such a comparison would not always be possible for local quantities because of quantum wave-packet spreading. Because of the presence of chaotic regions in the phase space, $C_{\mathrm{cl}}(t) \sim e^{2\tilde{\lambda}t}$ grows exponentially. Now we compare this classical CGR, $\tilde{\lambda} = \lim_{t\to\infty}\lim_{\Delta x(0)\to 0}(1/2t) \ln\{[C_{\mathrm{cl}}(t+1)]/[C_{\mathrm{cl}}(1)]\}$, to the standard definition of the LE: $\lambda = \langle\langle \lim_{t\to\infty}\lim_{d(0)\to 0}(1/t)\ln[d(t)/d(0)]\rangle\rangle$ [34] (where $d(t) = \sqrt{[\Delta x(t)]^2 + [\Delta p(t)]^2}$). Notice that there are key differences between the definitions of λ and $\tilde{\lambda}$ coming from the different orders of squaring, averaging, taking a ratio, and applying a logarithm.

Next, we proceed to check if the classical correspondence follows through in a quantum calculation of $C(t)$ and compare the rate of exponential growth of $C(t)$ to $\tilde{\lambda}$ extracted from $C_{\mathrm{cl}}(t)$ and to the LE λ. For the quantum case, the averaging in Eq. (2) is performed in the Schrödinger picture over some initial state $|\Psi(0)\rangle$. We use individual angular-momentum eigenstates $|\Psi(0)\rangle = |n\rangle : \hat{p}|n\rangle = \hbar_{\mathrm{eff}} n|n\rangle$ and Gaussian wave packets:

$$|\Psi(0)\rangle = \sum_{n=-\infty}^{\infty} a_n^{(0)}|n\rangle, \qquad a_n^{(0)} \sim \exp\left(-\frac{\hbar_{\mathrm{eff}}^2(n-n_0)^2}{2\sigma^2}\right), \tag{4}$$

where $n_0 = p_0/\hbar_{\mathrm{eff}}$. In this calculation, we use wave packet (4) with $p_0 = 0$ and $\sigma = 4$. Numerically, $|\Psi\rangle$ is represented in a finite basis of eigenstates $|n\rangle$, $n \in [-N; N-1]$. All functions of only $\hat{p}$ are applied in this basis, and all functions of only $\hat{x}$ are applied in the Fourier-transformed representation. We use an adaptive grid with $2\hbar_{\mathrm{eff}}N \in [2^7; 2^{16}]$ so that all physical observables are well converged. The wave function is evolved by switching between representations back and forth and applying the Floquet operator $\hat{F} = e^{-i\hat{p}^2/2\hbar_{\mathrm{eff}}}e^{-iK\cos(\hat{x})/\hbar_{\mathrm{eff}}}$ in parts. Then the correlators are calculated in the Schrödinger picture.

The exponential growth of $C(t)$ lasts between the time t_d and the Ehrenfest time t_E [3,14]. To achieve a hierarchical separation between t_d and t_E ($(t_E/t_d) \gg 1$) for the QKR, we have to tune both K and $\hbar_{\mathrm{eff}}$. The estimates of $t_d \sim [\ln(K/2)]^{-1}$ and $t_E \sim \{[|\ln\hbar_{\mathrm{eff}}|]/[\ln(K/2)]\}$ at $K > 4$ guide our choice of parameters to achieve this separation.

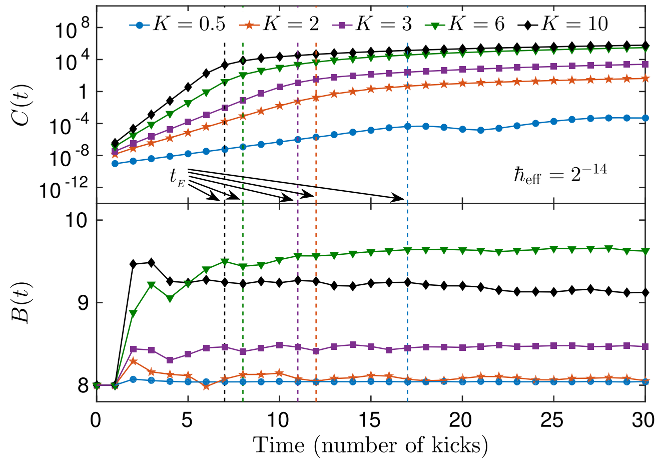

FIG. 1. The upper panel shows the OTOC $C(t)$ vs t in the semilog scale for various values of the kicking strength ($K = 0.5$, 2, 3, 6, 10) and $\hbar_{\rm eff} = 2^{-14}$. The lower panel is a plot of the two-point function $B(t)$ vs t at the corresponding parameters (in the linear scale). Averaging is performed over the Gaussian wave packet defined in Eq. (4) with $p_0 = 0$ and $\sigma = 4$.

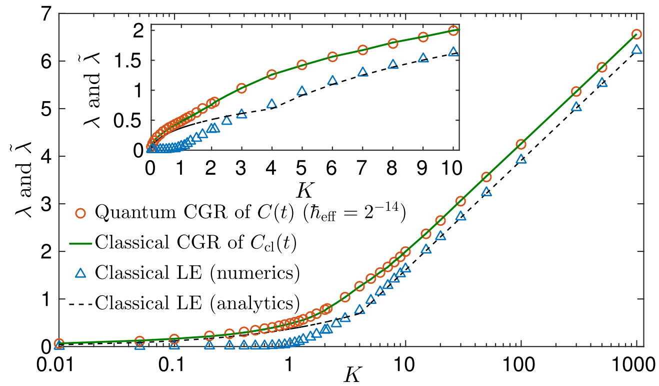

FIG. 2. Red circles: Early-time growth rate of $C(t)$ at $\hbar_{\rm eff} = 2^{-14}$ (quantum CGR). The rest of the data are classical. Green solid line: Growth rate of $C_{\rm cl}(t)$ (classical CGR). Blue triangles: LE calculated numerically. Black dashed line: LE according to the Chirikov analytical formula (5). The main plot and the inset show the same data in the lin-log and linear scales, respectively (and in different ranges). At $K \gtrsim 8$, the difference between the CGR and the LE is constant $\approx \ln\sqrt{2}$. The initial state in $C(t)$ is the Gaussian (4) with $p_0 = 0$ and $\sigma = 4$. Fitting details for extracting the CGR from $C(t)$ and $C_{\rm cl}(t)$ are given in the main text.

The smallest $\hbar_{\rm eff}$ within the scope of our numerics is $\hbar_{\rm eff} = 2^{-14}$. For this value of $\hbar_{\rm eff}$, the Ehrenfest time is in the range $7 \lesssim t_E \lesssim 17$ kicks for the range of kicking strength $0.5 \leq K \leq 10$. By $K = 1000$, t_E shrinks down to three kicks, but, at these values of K, it appears to be enough to extract a well-averaged exponent. For the above-mentioned parameter regimes, we numerically observe the exponential growth of $C(t)$ at early times ($t < t_E$) as shown in Fig. 1, upper panel. Figure 1 also shows that t_E decreases upon increasing the kicking strength K for fixed $\hbar_{\rm eff}$. In contrast to $C(t)$, the two-point correlator $B(t)$ saturates at time $t \sim 2$ kicks (Fig. 1, lower panel).

Equipped with the early-time behavior of $C(t)$, we are in a position to extract the rate of its exponential growth, i.e., obtain the CGR from the quantum calculation. We carry out a four-pronged comparison between the CGR from the quantum calculation of $C(t)$, the CGR from the classical calculation of $C_{\rm cl}(t)$, the numerically obtained LE for the KR, and analytical estimates (5) of the LE from Chirikov's standard map analysis [24]. Chirikov's analytical formula reads

$$\lambda \approx \frac{1}{2\pi}\int_{-\pi}^{\pi} dx \ln L(x), \tag{5}$$

where

$$L(x) = \left|1 + \frac{k(x)}{2} + {\rm sgn}[k(x)]\sqrt{k(x)\left(1 + \frac{k(x)}{4}\right)}\right| \tag{6}$$

and $k(x) = K\cos x$. The simplified expression $\lambda \approx \ln(K/2)$ valid at large K is obtained by substituting $L(x) \approx |k(x)|$ into Eq. (5) [24,34].

In Fig. 2, we compare the exponents obtained in four ways listed above. In order to extract the exponents from $C(t)$, we determine the times, after which the exponential growth starts slowing down, and fit $C(t)$ from $t = 1$ up to these times to the function $ae^{2\lambda_{\rm fit}(t-1)}$ to find the parameter $\lambda_{\rm fit}$ [$C(0) = 0$, so we omit $t = 0$]. Numerical calculations of the classical LE and of the classical CGR [i.e., the growth rate of $C_{\rm cl}(t)$] are performed using the map tangent to the standard map—this standard procedure is outlined in Supplemental Material [34]. Notice that the exponents extracted from $C(t)$ (quantum CGR) and from $C_{\rm cl}(t)$ (classical CGR) are in excellent agreement for all values of K. Both classical and quantum CGRs significantly exceed the LE at $K < K_{\rm cr}$. This indicates that the CGR may not be a reliable tool for discriminating between classically regular and chaotic dynamics in a global sense, but it can be employed to detect the existence of local disconnected chaotic islands more efficiently than the LE. As expected, numerically calculated values and analytical estimates of the classical LE agree with each other for $K \gtrsim 3$. At large K, the difference between the CGR and LE becomes nearly constant $\approx \ln\sqrt{2}$. We attribute this distinction primarily to the difference in the order of averaging in the CGR and LE.

Now we proceed to consider the deviation of $C(t)$ from its classical counterpart $C_{\rm cl}(t)$ that manifests sharply at a time close to t_E. The onset of this deviation in the OTOC is closely related to the weak dynamical localization effects [19]. In Fig. 3, we plot $\ln[C(t)]/2t$ as a function of time t in the log-log scale. This plot is constant [corresponding to the exponential rise of $C(t)$] at early times. Beyond t_E, the exponential growth slows down to a power-law growth

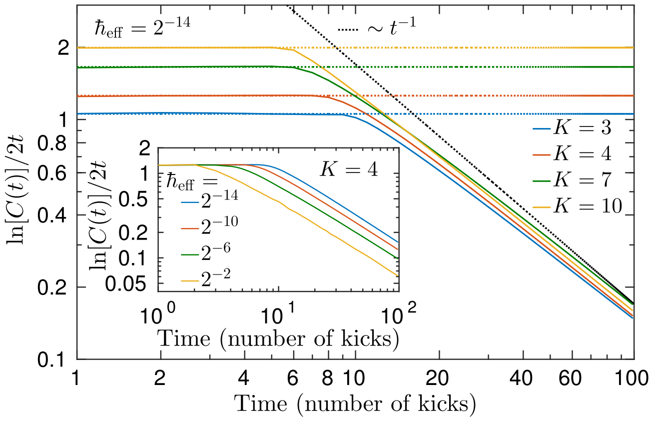

FIG. 3. Main plot: $\ln[C(t)]/2t$ vs t in the log-log scale for $K = 3$, 4, 7, 10 (from bottom to top line, respectively) and $\hbar_{\rm eff} = 2^{-14}$. The flat region at early times quantifies the exponential growth rate of $C(t)$. This flat region persists up to time t_E, at which the exponential growth slows down to a power-law growth with a slowly decreasing power. Dotted lines are guides to the eye: Horizontal lines extend the flat regions, and the sloped line is shown for a power comparison. Inset: $\ln[C(t)]/2t$ vs t in the log-log scale for $K = 4$ and $\hbar_{\rm eff} = 2^{-14}, 2^{-10}, 2^{-6}, 2^{-2}$ (from top to bottom line, respectively). The rate of exponential growth is the same for different values of $\hbar_{\rm eff}$, but t_E shrinks when $\hbar_{\rm eff}$ increases.

(nearly quadratic growth around $t \sim 100$ kicks). At long times, the growth of $C(t)$ slows down further, but numerics quantifying this slowdown is out of the scope of the present Letter. However, we can unambiguously extract the exponent associated with the exponential growth prior to t_E. Note that, in the range of K and $\hbar_{\rm eff}$ where the region of the exponential growth of $C(t)$ is present ($t_E \geq 3$), $\tilde{\lambda}$ does not depend on $\hbar_{\rm eff}$ (see Fig. 3, inset).

Regular-to-chaotic transition in long-time quantum dynamics.—The classical KR is famous for its transition from regular motion to chaotic behavior that occurs as K is increased above $K = K_{\rm cr} \approx 0.97$. The chaotic phase is characterized by the quasirandom walk in the angular-momentum space that leads to diffusion in angular momentum, so that the rotor's energy averaged over the phase space grows linearly with time (number of kicks). On the other hand, at long times the QKR undergoes dynamical localization (which is closely connected to Anderson localization in disordered solids [8]), and around $\hbar_{\rm eff} \sim 1$, the standard diagnostic—the average energy, i.e., the one-point correlator—seems insensitive to the presence or absence of classical chaos [1,4]. Thus a question arises: Is there a quantum diagnostic that manifests a robust signature of a regular-to-chaotic classical transition in the purely quantum dynamics even in the dynamically localized regime ($\hbar_{\rm eff} = 1$, $t_d \gg t_E$)? Remarkably, the two-point correlator [$B(t)$ in Eq. (2)] contains a sharp signature of the classical transition [35]. In particular, we consider $B(t)$ averaged over time within various windows τ:

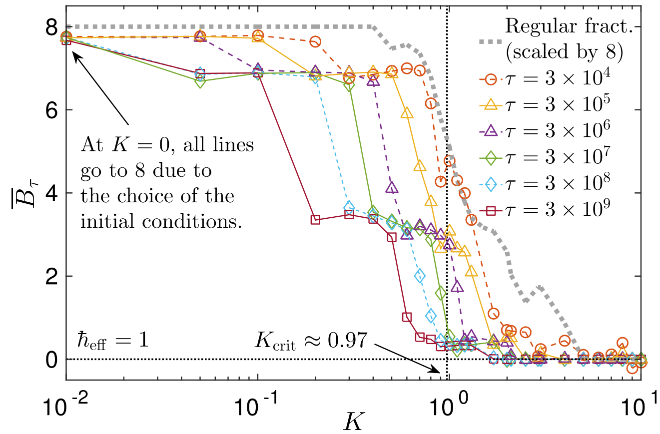

FIG. 4. Long-time average $\bar{B}_\tau$ (7) (over various windows τ) of the two-point correlator $B(t)$ as a function of K compared to the regular fraction of the phase space weighted with the initial Wigner distribution $P(x, p)$ (scaled). The trend with increasing τ shows that, at all $K \neq 0$, the correlations decay in time, but the rate of this decay has a steplike dependence on K. At $K > K_{\rm cr}$, the decay is quite fast, while at $K < K_{\rm cr}$, it takes $\bar{B}_\tau$ at least an exponentially large window to vanish. It is not clear from the data whether at small $K \neq 0$ the averaged correlator eventually goes to zero at $\tau \to \infty$ or is bounded from below. The initial state corresponding to $P(x, p)$ is the Gaussian (4) with $p_0 = 0$ and $\sigma = 4$.

$$\overline{B}_\tau = \frac{1}{\tau} \sum_{t=0}^{\tau} \mathrm{Re}\langle p(t) p(0) \rangle. \tag{7}$$

As shown in Fig. 4, this averaged correlator maintains a sharp steplike structure as a function of K for several orders of magnitude in τ (we reached as large a window as $\tau = 3 \times 10^9$, which is many orders of magnitude longer than any characteristic time scale in the system). This implies that, at very long times, the quantum system does not lose

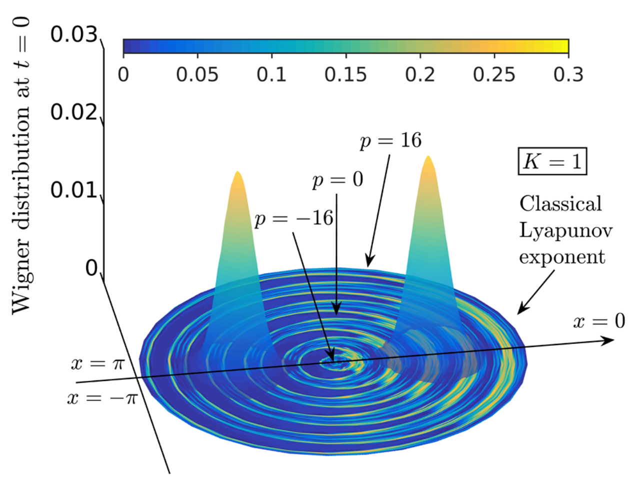

FIG. 5. Initial Wigner distribution $P(x, p)$ (3D plot) on the top of the classical Lyapunov exponent (shown in color in the horizontal plane; see the color bar for numerical values). The initial state corresponding to $P(x, p)$ is the Gaussian (4) with $p_0 = 0$ and $\sigma = 4$. The Lyapunov exponent is shown for $K = 1$.

the information about the classical transition. The plot supports the following very intuitive statement. The larger the chaotic fraction of the classical phase space is, the shorter the correlation-decay time window becomes (for an explicit demonstration of this behavior, the dependence of $\overline{B}_\tau$ on the averaging window size τ is given in Fig. S2 in Supplemental Material [34]). Therefore, we can relate $\overline{B}_\tau$ to the regular part of the phase space weighted by the initial Wigner distribution $P(x,p)$ of QKR (see Fig. 5 for an illustration). However, $\overline{B}_\tau$ keeps decaying with time, while the regular phase-space fraction is a constant determined by the initial conditions and K, so a fixed window should be chosen for a comparison. As the ratio of regular to chaotic areas of the phase space decreases, so does the average value of the correlator over this window, until it reaches zero at large K, where almost no regular regions are present.

E. B. R. and V. G. were supported by NSF-DMR 1613029 and the Simons Foundation. S. G. gratefully acknowledges support by LPS-MPO-CMTC, Microsoft Station Q. E. B. R. and V. G. are grateful to Shmuel Fishman for discussions and valuable comments. S. G. acknowledges valuable discussions with A. G. Abanov and D. Huse. V. G. is grateful to Chushun Tian and Hui Zhai for valuable discussions and hospitality at the Institute for Advanced Study, Tsinghua University, where a part of this work was completed.

*efimroz@umd.edu

[1] G. Casati, B. Chirikov, F. Izraelev, and J. Ford, in *Stochastic Behavior in Classical and Quantum Hamiltonian Systems*, Lect. Notes Phys. Vol. 93, edited by G. Casati and J. Ford (Springer, Berlin, 1979), pp. 334–352.
[2] D. L. Shepelyansky, Physica D (Amsterdam) **8**, 208 (1983); G. Casati, B. V. Chirikov, I. Guarneri, and D. L. Shepelyansky, Phys. Rev. Lett. **56**, 2437 (1986); T. Dittrich and R. Graham, Ann. Phys. (N.Y.) **200**, 363 (1990).
[3] G. Berman and G. Zaslavsky, Physica A (Amsterdam) **91**, 450 (1978); M. Berry, N. Balazs, M. Tabor, and A. Voros, Ann. Phys. (N.Y.) **122**, 26 (1979).
[4] B. V. Chirikov, F. M. Izrailev, and D. L. Shepelyansky, Sov. Sci. Rev. Sect. C **2**, 209 (1981).
[5] B. V. Chirikov, F. M. Izrailev, and D. L. Shepelyansky, Physica D (Amsterdam) **33**, 77 (1988).
[6] M. V. Berry, Les Houches Lect. Ser. **36**, 171 (1983).
[7] F. Haake, M. Kuś, and R. Scharf, Z. Phys. B **65**, 381 (1987); F. Haake, *Quantum Signatures of Chaos*, 3rd ed. (Springer-Verlag, Berlin, 2010), Vol. 54.
[8] S. Fishman, D. R. Grempel, and R. E. Prange, Phys. Rev. Lett. **49**, 509 (1982); D. R. Grempel, S. Fishman, and R. E. Prange, Phys. Rev. Lett. **49**, 833 (1982); R. E. Prange, D. R. Grempel, and S. Fishman, Phys. Rev. B **29**, 6500 (1984).
[9] M. Toda and K. Ikeda, Phys. Lett. A **124**, 165 (1987).
[10] F. Haake, H. Wiedemann, and K. Życzkowski, Ann. Phys. (N.Y.) **504**, 531 (1992).
[11] R. Alicki, D. Makowiec, and W. Miklaszewski, Phys. Rev. Lett. **77**, 838 (1996).
[12] I. L. Aleiner and A. I. Larkin, Phys. Rev. B **54**, 14423 (1996); Phys. Rev. E **55**, R1243 (1997); O. Agam, I. Aleiner, and A. Larkin, Phys. Rev. Lett. **85**, 3153 (2000).
[13] A. Kitaev, KITP, http://online.kitp.ucsb.edu/online/entangled15/kitaev/.
[14] J. Maldacena, S. H. Shenker, and D. Stanford, J. High Energy Phys. 08 (2016) 106.
[15] A. Larkin and Yu. N. Ovchinnikov, Zh. Eksp. Teor. Fiz. **55**, 2262 (1969) [Sov. Phys. JETP **28**, 1200 (1969)].
[16] B. Swingle, G. Bentsen, M. Schleier-Smith, and P. Hayden, Phys. Rev. A **94**, 040302 (2016); B. Swingle, M. D. Lukin, D. M. Stamper-Kurn, J. E. Moore, and E. A. Demler, arXiv:1607.01801.
[17] Y. Huang, Y.-L. Zhang, and X. Chen, Ann. Phys. (Berlin), DOI: 10.1002/andp.201600318 (2016); Y. Chen, arXiv:1608.02765; B. Swingle and D. Chowdhury, arXiv:1608.03280; R. Fan, P. Zhang, H. Shen, and H. Zhai, arXiv:1608.01914.
[18] F. M. Izrailev and D. L. Shepelyansky, Teor. Mat. Fiz. **43**, 417 (1980) [Theor. Math. Phys. **43**, 553 (1980)].
[19] C. Tian, A. Kamenev, and A. Larkin, Phys. Rev. Lett. **93**, 124101 (2004).
[20] W. K. Hensinger, H. Haffner, A. Browaeys, N. R. Heckenberg, K. Helmerson, C. McKenzie, G. J. Milburn, W. D. Phillips, S. L. Rolston, H. Rubinsztein-Dunlop, and B. Upcroft, Nature (London) **412**, 52 (2001).
[21] D. A. Steck, W. H. Oskay, and M. G. Raizen, Science **293**, 274 (2001).
[22] G. B. Lemos, R. M. Gomes, S. P. Walborn, P. H. S. Ribeiro, and F. Toscano, Nat. Commun. **3**, 1211 (2012).
[23] J. Larson, B. M. Anderson, and A. Altland, Phys. Rev. A **87**, 013624 (2013).
[24] B. V. Chirikov, Phys. Rep. **52**, 263 (1979).
[25] A. Peres, Phys. Rev. A **30**, 1610 (1984).
[26] H. Pastawski, P. Levstein, G. Usaj, J. Raya, and J. Hirschinger, Physica A (Amsterdam) **283**, 166 (2000).
[27] P. Jacquod, P. G. Silvestrov, and C. W. J. Beenakker, Phys. Rev. E **64**, 055203 (2001).
[28] R. A. Jalabert and H. M. Pastawski, Phys. Rev. Lett. **86**, 2490 (2001).
[29] F. M. Cucchietti, C. H. Lewenkopf, E. R. Mucciolo, H. M. Pastawski, and R. O. Vallejos, Phys. Rev. E **65**, 046209 (2002).
[30] F. M. Cucchietti, H. M. Pastawski, and D. A. Wisniacki, Phys. Rev. E **65**, 045206 (2002).
[31] S. Chaudhury, A. Smith, B. E. Anderson, S. Ghose, and P. S. Jessen, Nature (London) **461**, 768 (2009).
[32] I. García-Mata and D. A. Wisniacki, J. Phys. A **44**, 315101 (2011).
[33] See Fig. S1 in Supplemental Material at http://link.aps.org/supplemental/10.1103/PhysRevLett.118.086801 for a comparison between $C(t)$ and $C_{\mathrm{cl}}(t)$.
[34] See Supplemental Material at http://link.aps.org/supplemental/10.1103/PhysRevLett.118.086801 for details on the definition and calculation of the classical Lyapunov exponent.
[35] In addition, the time dependence of $B(t)$ in the interval $t \in [0, t_{\max}]$ is much more accessible than that of the OTOC $C(t)$, as their computation complexities scale as $O(t_{\max})$ and $O(t_{\max}^2)$, respectively.